Advances in obsidian hydration dating by secondary ion mass spectrometry: World examples

I. Liritzis *, N. Laskaris

University of the Aegean, Dept. of Mediterranean Studies, Laboratory of Archaeometry, 1 Demokratias Ave., Rhodes 85100, Greece

A B S T R A C T

Since 1960 the potential of obsidian as a chronometer in archaeology has been subjected to several drawbacks and studies. While economical, simple and fast, obsidian hydration dating today is generally unreliable. A novel approach towards obsidian hydration dating, named SIMS-SS, has recently been initiated based on modelling the hydrogen profile acquired by secondary ion mass spectrometry (SIMS), following Fick's diffusion law, and the rationale of surface saturation (SS) with water molecules. The new nuclear method is presented with significant refinement regarding numerical calculation of age parameters, the suitability criteria of the sampling area and the spectral shape of the concentration dependant H^+ profile. A reappraisal is applied to thirteen obsidian specimens from all over the world ranging some 100's to 30,000 years old. The results reinforce the precision and reliability of the SIMS-SS method, enhancing its wide applicability.

© 2008 Elsevier B.V. All rights reserved.

1. Introduction: a brief historical overview

Obsidian hydration dating (OHD) has been a part of the archaeological analytical toolbox for nearly four decades. However, the reported ages have been variously assigned as either highly uncertain or sound for several other archaeological applications.

The first report of OHD was by Friedman and Smith [1]. They noted that (a) the exposed surfaces of ancient obsidian artefacts had absorbed water, (b) the hydration birefringent rims were visible under high-power magnification (approximately 500×), and (c) its width was dependent on time, chemical composition (obsidian source), and temperature. This hydration process converts a hydration layer of a measured thickness to an absolute date with an established rate for the inward diffusion of molecular water using the equation:

$$x = (kt)^{1/2}, \tag{1}$$

where x is the hydration rim width in microns, k is the hydration rate at a particular temperature/relative humidity, and t is time.

Two major tasks in Eq. (1) are to determine the thickness x and the value of k for specific archaeological site conditions.

The rim was initially measured by optical microscopy [1,2], but inaccuracies in the determination of the end point of the water front [3] lead to measurements with other non-optical techniques, such as nuclear reaction analysis, infrared photoacoustic spectroscopy and SIMS [3–9]. The diffusion coefficient was estimated from the rate at high temperature (160 °C) and extrapolation to ambient site conditions using the Arrhenius equation [2,3,10].

Research subsequent to Friedman and Smith's original presentation has refined the method into two distinct techniques. The simplest, which is referred to as 'empirical rate dating' [11–14], requires correlating the width of optically measured rims to independent chronometric data, such as ^{14}C [15]. The second, more complex and widely applied, is known as 'intrinsic rate dating' and requires experimentally determined rate constants and a measurement of the site temperature because it is theoretically a fully independent chronometric method [2,10,16–18].

The mathematical model utilized in the intrinsic rate OHD is

$$x^2 = At e^{-E/RT}, \tag{2}$$

where x is the depth, A is a constant, E is the activation energy, R is the gas constant, and T temperature. Nevertheless, the assumptions

* Corresponding author. Tel.: +30 22410 99385; fax: +30 22410 99320.
E-mail address: liritzis@rhodes.aegean.gr (I. Liritzis).

made by Eq. (2) are proved incorrect from the sigmoid hydrogen profiles measured by SIMS. Moreover, along with the so-called 'intrinsic' method, the importance of connate water, the compositional indices and density, in controlling the hydration rate of obsidians has been demonstrated by several authors [19–21].

In spite of over 40 years of development and application, neither method has produced consistently reliable results. In some cases ages have so contradicted other well-established chronometric data that the utility of the obsidian as a chronometer has been questioned [9,22–26].

The problems with OHD are due to the use of inappropriate analytical techniques, which involve non-systematic errors arising from them, the inherent imprecision of optical measurements, the experimental conditions of the estimation of hydration rate, and an improper model of the hydration process. The scientific background has illustrated the complexity of the hydration process and revised working assumptions for OHD have been proposed [9,15,10,17,20,25]. A 70% failure has been estimated in conventional OHD [9,25,18].

A further advancement of OHD with a completely new rationale – the monitoring of hydrogen profile in obsidian surfaces – suggests that refinement of the OHD technique is possible in a manner which improves both its accuracy and precision and potentially expands the utility by generating chronological, as well as, paleoenvironmental data. An earlier attempt using nuclear reactions to monitor H⁺ by depth was not followed up [27], while the role of SIMS in cultural heritage studies has been evaluated [28].

2. The novel SIMS approach

Two groups (ours in Rhodes and another from Tennessee, Oak Ridge) initiated the use of SIMS for dating purposes. Anovitz et al. [9] presented a model of the sigmoid curve which relied solely on compositionally-dependent diffusion, following numerical solutions (finite difference, FD, or finite element). A test followed this technique using results from Mount 65, Chalco in Mexico [25]. This technique uses numerical calculation to model the formation of the entire diffusion profile as a function of time and is fitted to the profile as a whole (excluding the near-surface region). Here the solution involves a number of assumptions, including boundary conditions and the nature of the actual diffusion process, so that only appropriate diffusion equations could be selected. Moreover, the diffusion coefficient D (m² s⁻¹) was empirically determined, but for some combinations of D, time step Δt and depth step Δx, an explicit solution became numerically unstable. In general, the FD equations are based on a number of assumptions about the behaviour of water as it diffuses into glass. Therefore, in their report several assumptions and calibration requirements were made, based upon characteristic points of the SIMS H + diffusion profile.

At the same time Liritzis and Diakostamatiou [8] promoted a different concept of obsidian surface saturation with diffusion water and introduced an alternative phenomenological approach of SIMS-SS. The H⁺ profile was best fitted by a 3rd order polynomial, D was taken as the inverse of the first derivative of the S-shape, and varied with an exponential dependence of the concentration C, and based on Fick's Second Law and Boltzmann's transformation involving auxiliary variables and boundary conditions, the diffusion time (t) that corresponds to the entire profile was found in relation to D and C at the surface saturation (SS) layer [26]. Subsequent works on the theoretical background underlying the SIMS-SS method, as well as some experimental and surface assessments have strengthen its validity [21,29–31].

The rationale of the SIMS-SS dating method is based on modelling of the diffused water profile, especially along the first 1–10 μm. Very important in our diffusion age modeling is the formation of a saturation layer near the exterior of the surface. In fact,

since the cutting of an artefact by prehistoric man, water from ambient humidity enters rapidly and presumably perpendicular to the obsidian's surface. In the first 1–5 μm diffusion is faster and saturation occurs, while, subsequently a slower diffusion continue from this layer onwards to the interior of the blade. This saturation layer is formed by the difference between the rates of the two diffusions.

The age calculation is separated into two major steps. First, is the calculation of a 3rd order fitting polynomial (Eq. (3)) of the SIMS profile. Second is the determination of the saturation layer, i.e. its depth and concentration. These two major steps are accompanied by the calculation of the first derivative of the polynomial, the calculation of a first derivative of a second polynomial that fits the hydration profile from the beginning until the inflection point. All these calculations are embedded in software created in Matlab with a windows environment and an application executable under Windows XP. The software is briefly described in section 4[1].

The software uses the age equation proposed earlier [8] (Eq. (4)) in order to calculate the age in years

$$C = e^{a+bx+cx^2+dx^3}, \tag{3}$$

$$T = \frac{(C_i - C_s)^2 \left(\frac{1.128}{1 - \frac{0.177kC_i}{C_s}} \right)^2}{4D_{s,eff} \left(\frac{dC}{dx}\big|_{x=0} \right)^2}, \tag{4}$$

where, C_i is the intrinsic concentration of water, C_s is the saturation concentration (atoms/cc converted to g mols/cc), dC/dx is the diffusion coefficient for depth $x = 0$, k is derived from a family of Crank's theoretical diffusion curves [32], and $D_{s,eff}$ is an effective diffusion coefficient (Eq. (5)) which relates the inverse gradient of the fit polynomial to well dated samples:

$$D_{s,eff} = a^*D_r + b/(10^{22}D_r), \text{ where, } D_r = (1/(dC/dx)) \times 10^{-11}. \tag{5}$$

3. SIMS equipment and measurements

The SIMS technique consists simply of bombarding a solid with a focused ion beam within a vacuum chamber and detecting the ions emitted from the surface using a mass spectrometer. Analyses for H⁺ in present work are made in a quadrupole instrument which typically uses a Cs beam and no conductive coating is needed. The primary ion beam having a current of several nA to 100's of nA is focused to a beam size of microns to 10's of microns. For the H⁺ depth profiling acquired on hydrated obsidians raster-scanned by the beam and secondary ions accepted into the mass spectrometer must be limited to those emitted from the central part of the crater. Ion acceptance is done by electronic gating. Typically less than 40% of the rastered area is used as the acceptance area for analysis. Charge build-up is compensated with electron bombardment, eliminating the need to coat the samples with a conductive layer. Hydrogen atoms/cc are thus collected as a function of crater depth which form a sigmoid curve. The present dynamic SIMS measurements were carried out using Phi 6300 and 6600 quadrupole-based SIMS instruments. Samples are held by clips and screws to minimize damage, but occasionally also with silver paste where they are typically dried in an oven for 30–60 min at 60–80 °C. No gold or other conductive coating is applied to the samples, in contrast to methods published for magnetic sector SIMS instruments [9,25].

Profiles were acquired using Cs bombardment, typically with a 5 keV energy and an incidence angle of 60° relative to the surface normal. The ion beam current is typically 500–800 nA. The system

---

[1] A free demonstration and use is made available in http://www.rhodes.aegean.gr/tms/sims-ss, provided that appropriate citation is made to the website and present paper.

has a base pressure of 7×10^{-10} Torr i.e. achieved when the ion and electron gun are not operating, and the typical operating pressure is about 2×10^{-9} Torr, usually achieved within about 15 min of sample introduction. In fact when operating, both the electron gun and ion gun raise the chamber pressure, so the operating pressure is higher during analysis. For analysis of low hydrogen contents in obsidians, the chamber pressure is determines what background can be achieved. However in the case where we are analyzing samples containing percent levels of hydrogen in them the chamber pressure has little effect on the background achieved. In fact the chamber pressure has little effect on the accuracy of the analysis either, as accuracy is controlled by how closely the analysis conditions are replicated between the standard and the unknown. Because the sample stage can be adjusted in X, Y, Z and tilt, it is relatively easy to reproducibly position a reflective surface in the analysis position.

Typical SIMS depth profiles for H$^+$ in obsidian artefacts are given in Fig. 5. These sigmoid profiles show similar shapes in having a thin surface layer in which the hydrogen content falls sharply, fol-lowed by a more gradually sloped profile that may extend many microns into the sample, depending on the age of the artefact [21]. Finally the H$^+$ profile falls sharply at some depth which is also dependant on the age of the artefact. The surface peak may, at least partially, result from the large adsorbed water layer detected on every air-exposed surface. However, even smooth polished laboratory-hydrated obsidian and glass samples show this surface peak, suggesting it is a fundamental feature of water diffusion into obsidian occurring during sputtering, accounting for any other possible cation depletion too [37,38].

Conversion of sputtering time to depth in SIMS profiles is typically done by measuring the analytical crater depths using a stylus profilometer. Repeat measurements of calibration standards have demonstrated that the stylus profilometer itself is precise to within 1%. A round robin study of profilometry measurements of SIMS craters in *flat* (i.e. polished semiconductor) samples shows that this procedure is accurate to within 5% [33]. For hydrated obsidians, repeat measurements of polished samples have shown an error of 3% for flat samples [25]. However this latter procedure requires cut-
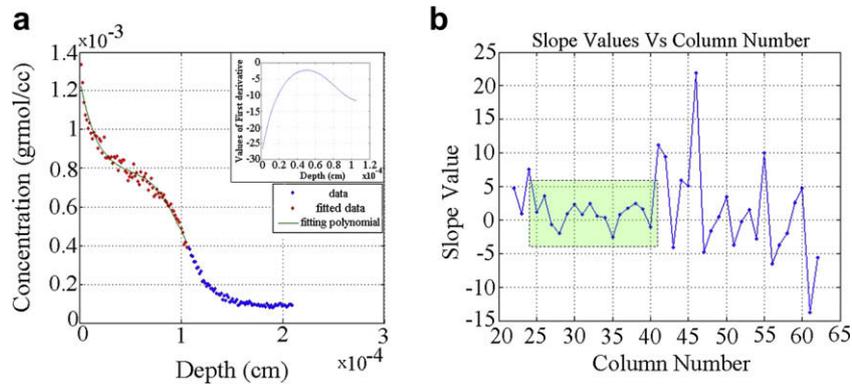

Fig. 1. (a) A 3rd order polynomial fitting at the diffused region of the SIMS profile. The 1st derivative of this is shown in the inset, (b) linear regression slopes versus data points. Green square is the saturation layer region.
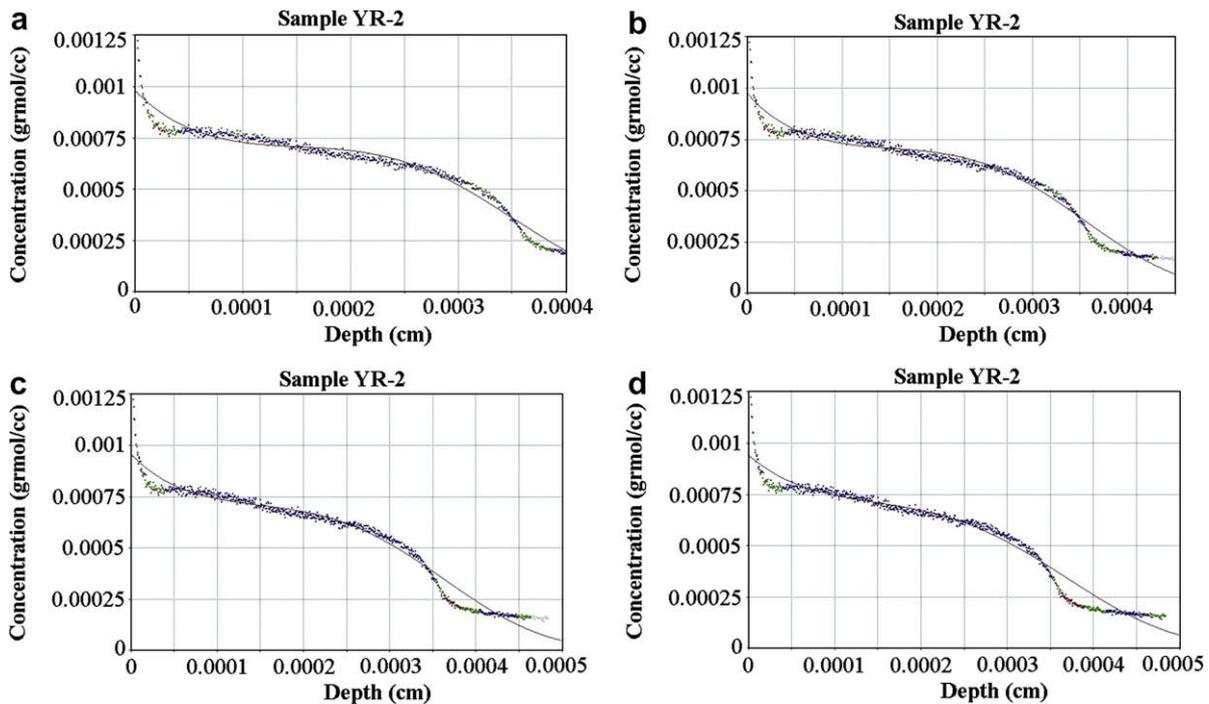

Fig. 2. The four main fittings for the calculation of the best 3rd order polynomial. (a) cut points no tail, (b) tail with 0.000025 cm added, (c) tail with 0.000060 cm added, and (d) tail with 0.000080 cm added.

ting and polishing a piece of material to ensure accurate measurements. Direct profilometry measurements can be made of craters on artefact surfaces. However roughness and tilt of typical artefact surfaces commonly have larger errors than flat polished surfaces [29,34]. Generally SIMS is accurate to within 5–10%, which translates to an estimated error of +/− 0.05 μm. This value is equivalent to +/−0.01–0.03 μm standard deviations associated with SIMS because of the irregular surfaces topography presented in naturally cleaved samples. As the surface of archaeological obsidian tool samples are generally smooth but typically curved, any strong field gradient is greatly affected by the tilt and shape of the analysis surface, and small differences in sample positioning may greatly affect the analysis. However, in the quadrupole instrument the sample stage can be tilted to aid in sample positioning and the lower field gradient means that there is less effect due to curved sample surfaces.

In our work, calibration of the concentration and depth axes is made by using a deuterium-implanted high-silica non-hydrated obsidian (KSW-354) [35] as a standard material. The use of ion implanted standard materials is common for quantitative SIMS analyses in the semiconductor industry [36]. Calibration of the depth scale simply involves using the known peak depth of the implant, previously established by stylus profilometry, to calculate the sputtering rate for a given analytical run. The relative standard deviation is around 4% in stylus profilometer measurements alone. The standard is analyzed in each analytical run so as to correct for small variations in instrument conditions from run to run. The advantages of using this method include simplicity, avoiding cutting the sample and good reproducibility. Using this method for depth calibration avoids errors that may be introduced by stylus profilometer measurements of rough artefact surfaces.

An assessment of the variation in sputtering rate for different glasses have shown that these glasses have a 1 sigma relative standard deviation (RSD) of 3.6% of the average rate for all glasses [37,38].

4. Advancement in SIMS-SS dating procedure

The use of the nuclear method with the present advances is intended to enhance the reliability of this new chronological tool for OHD and establish its wide applicability to a variety of environments. Following the first initial tests, the present reappraisal refers to: (a) a safer and faster way to the determination of the surface saturation layer, (b) the improved, faster and effective numerical calculation of age parameters, (c) the application of certain suitability criteria about the sampling area, and (d) devising proper plotting criteria of parameters derived from H^+ profile spectral shape. These advanced investigations were applied to 13 new obsidian blades from all over the world.

The present reassessment has the following stages. For the determination of the saturation layer, the depth of the inflection point is initially determined. Theoretically this is the depth where silica reacts with water [39] according to

$$Si - O - Si + H_2O = SiOH + OHSi. \quad (6)$$

Estimation of this depth is made through use of the first derivative of a *cubic spline fitting* with the Savitzky–Golay algorithm. Subsequently, the fitting with a 3rd order polynomial is determined from the beginning of the SIMS profile up to the inflection depth. This facilitates the location of the 1st derivative of the polynomial fitting (see inset of Fig. 1(a)). Following this, a new fit from the beginning of the profile until this 1st derivative peak with a new 3rd order polynomial is computed and a new derivative is found. This procedure continues until the very beginning of the SIMS profile or a derivative with no peak is reached. Then, repeated linear regressions are run from the last found derivative peak to the peak of the initial 1st derivative. It was noticed that the saturation layer lies always between these two peaks. This way the SS layer is defined
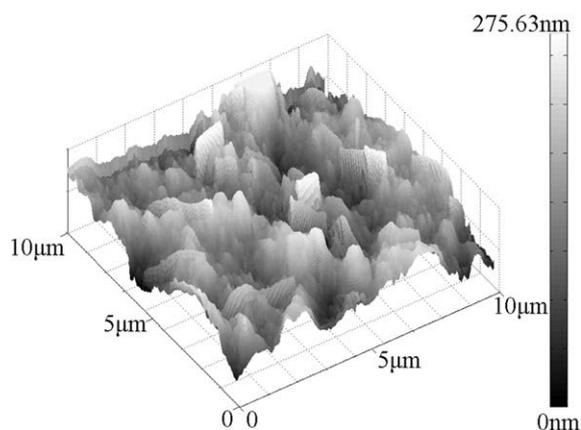

Fig. 4. AFM image of obsidian artefact from Sarakinos Cave, Greece. Note the roughness which appears in a 3D grey scale transformation of 2D image, indicating cracks, troughs, crystalline presence as white spots or elongations (confirmed also from PLM and SEM observation).
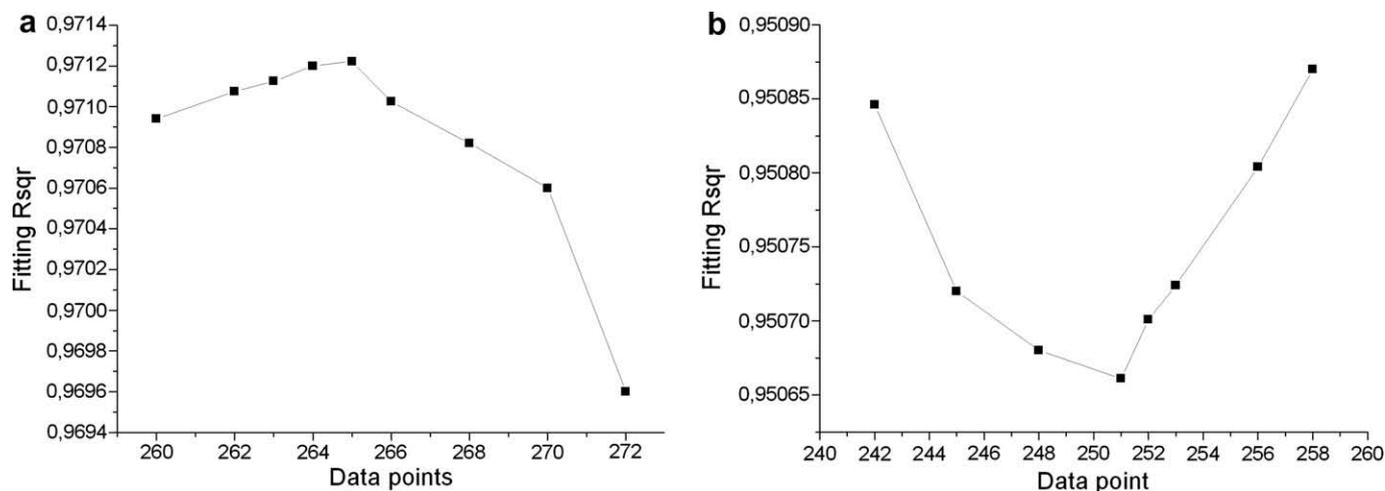

Fig. 3. Two types of bell-shaped hyperbola, (a) normal bell shape and (b) reversed bell shape. For both the number of data points used for choosing appropriate polynomial fit is 265 and 251 respectively.

much faster (an order of 30–60% in time elaboration) and more accurately compared to earlier sole use of the application of successive linear regressions to the whole SIMS profile [8]. At the end of this procedure a bi-plot of the linear regressions slope versus data points clearly defines the saturation layer (Fig. 1(b)).

A further assessment concerns the calculation of the 3rd order polynomial modelling of the hydrogen profile, a most crucial parameter that requires accurate statistical procedures. Here, the initial data points caused by sputtering effects of the ion beam are removed, and the fitting is repeated by cutting and adding data points in the tail. Initially the whole tail is cut and the first 3rd order polynomial fitting is obtained on the remaining profile (Fig. 2(a)). The tail end point and corresponding Rsqr of this fitting are recorded. Subsequently, successive single data points are added to the cut tail and the polynomial fitting is re-run. Following this the new Rsqr values are recorded. This procedure is repeated to the end of the tail (see, Fig. 2(b–d) with added depth points of 2.5–8 μm). In a few cases addition of extra points to the tail is made from the concentration value randomly selected from one of the last ten points of the flat section of C_i. A plot of Rsqr versus data point number is constructed which forms a bell-shape curve (Fig. 3). This bell-shaped curve, occasionally with a local maximum (Fig. 3(a)) or a local minimum (Fig. 3(b)), in fact, alludes to the suitable polynomial needed for further processing. At any rate, the 3rd order polynomial fit at the curving bell's turn is the optimum polynomial, which is used to compute the diffusion rate and the age.

The depth of the saturation layer (X_s) is calculated from the mean value of the depths of the layer, and the saturation concentration (C_s) is the mean value of the concentrations in the saturation segment. The intrinsic concentration (connate water, C_i) is found from the mean value of the last 10–20 data points of the tail. Finally, the saturation attributes is used to calculate the k parame-
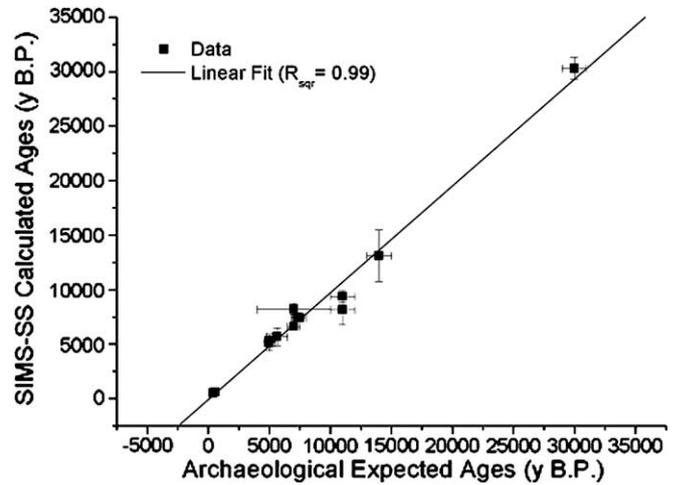

Fig. 6. Age calculated with SIMS-SS method versus expected ages calculated with various techniques (C-14, stratigraphy, etc.).

ter and then apply these parameters in the age equation (Eq. (4)), to compute the age along with the standard deviation (σ). σ is the standard deviation of the depth and the concentration made using Taylor's law for error propagation.

Elimination of random errors from the ion sputtering and surface roughness is achieved by the prior inspection of the artefact with Atomic Force Microscopy (Fig. 4). Noteworthy is the reported linear correlation between the surface roughness and the standard deviation of the saturation concentration confirming the correlation of these two factors [29].
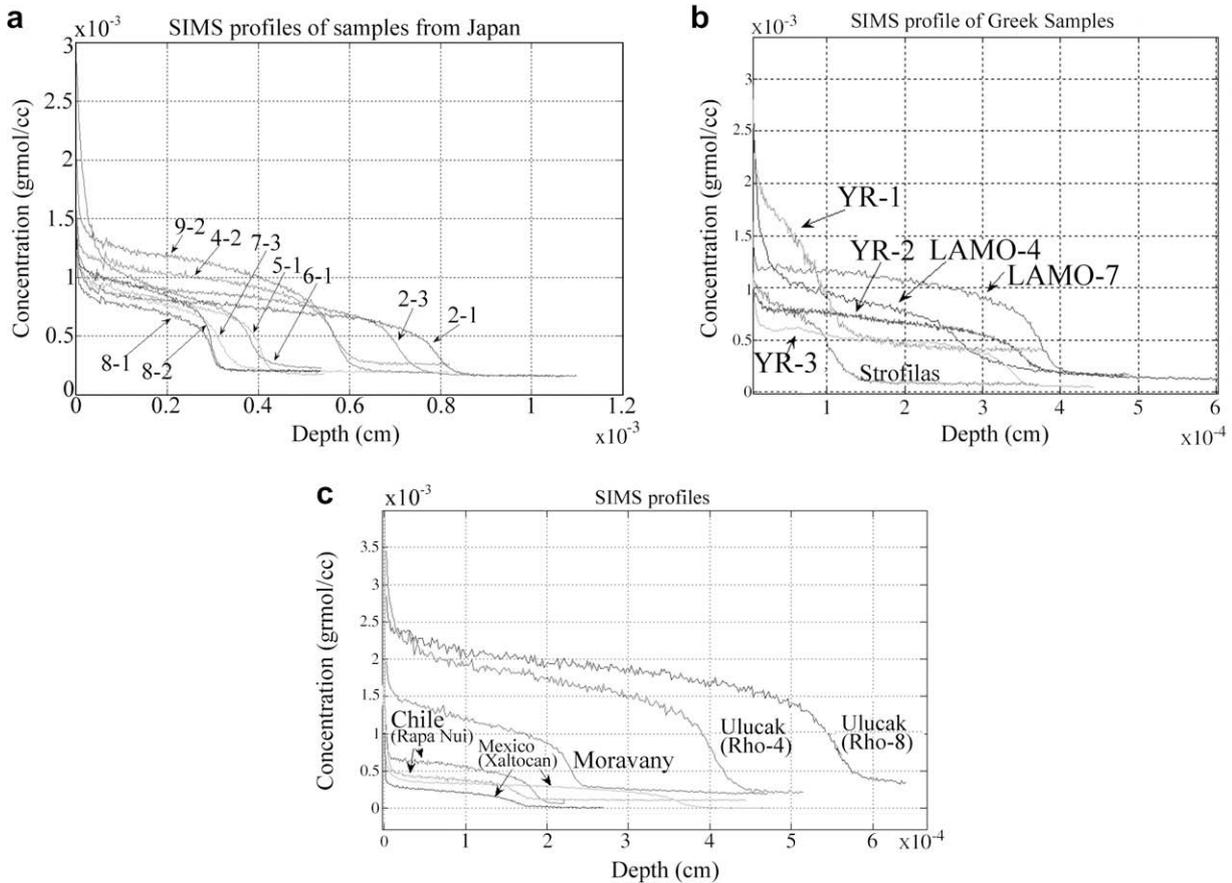

Fig. 5. SIMS profiles for 22 samples. (a) Japanese samples, (b) samples from Greece and (c) samples from other sites around the world.

Table 1
Samples analyzed with SIMS and dated by SIMS-SS ([*] by C-14 calibrated. SIMS profiles were made at Evans Analytical, thanks to Dr. S. Novak. Errors in the Japanese C-14 ages are 2–3% [**] archaeological typological sequences).

Location	Sample	X_s (cm)	C_s (g mol/cc)	C_i (g mol/cc)	e^k	D_s (cm²/year)	Age a BP	C-14 a BP
Japan	2-1, Dotegami, section de, Lower BBV	8.38e–5 ± 1.88e–6	0.0008566 ± 8.48e–6	0.0001622 ± 3.46e–6	290	1.2e–12	30294 ± 1014	30,000[*]
Japan	4-2, Kuzubara site, FBsc	0.0001884 ± 7.88e–6	0.00103 ± 9.73e–6	0.0002792 ± 6.25e–6	40	4.3e–13	13099 ± 2371	14,000[*]
Japan	6-1, Shimizu Yanagi Kita, KU	0.0001272 ± 2.98e–6	0.00098 ± 6.16e–6	0.00022 ± 3.1e–6	40	1.5e–12	7414 ± 182	7500[*]
Japan	8-1, Futatsudô, section a, KU	7.62e–5 ± 2.9e–6	0.000786 ± 6.89e–6	0.0002177 ± 8.07e–6	80	8.5e–13	5308 ± 601	5000[*]
Japan	8-2, Futatsudô, section a, KU	6.40e–5 ± 4.64e–6	0.00099 ± 1.26e–5	0.0002078 ± 4.41e–6	140	1.356e–12	5136 ± 738	5000[*]
Greece	Lamo-4, blade, D6067, Raches-Fournoi, Phthiotis	9.645e–5 ± 3.6e–6	0.00094 ± 2.6e–5	0.000121 ± 4.3e–6	40	3.14e–12	8193 ± 522	5000[**] Prehistoric (4000–10,000)
Greece	Stroflias-1-Andros Island, Aegean Sea (40520-11)/Dr. Chr. Televantou	5.01e–5 ± 6.6e–6	0.00078 ± 4.17e–5	7.65e–5 ± 8.58e–6	60	5.63e–12	5679 ± 819	4800–6500[**]
Greece	YR-2, Youra Island, Aegean Sea, (DL-2000-153), section Γ, layer 3, 1-7-93, A/A8	5.590e–5 ± 1.136e–6	0.0007864 ± 1.37e–5	0.00015893 ± 5.521e–6	280	1.45e–12	9368 ± 516	10,000–12,000
Greece	YR-3, Youra Island, Aegean Sea, 30-6-94, section Γa, layer 7, AA259	0.00010174 ± 4.781e–6	0.000543177 ± 5.9857e–6	5.5296e–5 ± 3.180e–6	50	4.29e–13	8141 ± 1346	10,000–12,000
Asia Minor	UlucaK, (RHO-4), CLG IVg, kindly supplied by Prof. Altan Çiliniroglou	0.0001743 ± 3.199e–6	0.001831 ± 3.97e–6	0.0002148 ± 1.16e–5	20	5.74e–13	6620 ± 348	6000–8000[*]
Chile Rapa Nui	1993-82, kindly supplied by Dr. C. Stevenson (re-evaluated)	4.94e–5 ± 2.94e–6	0.000418 ± 1.09e–5	0.0001082 ± 4.42e–6	40	1.07e–12	514 ± 90	310–522[*]
Hungary	Moravany-3, trench F, sector 3/2001, sq, 8, feature 3/01 depth 70-80 cm (40102-33)/ Prof. Janusz Kozlowski, Poland	5.47e–5 ± 3.95e–6	0.001344 ± 2.36e–5	0.0002004 ± 5.74e–6	140	3e–12	7423 ± 346	7300 ± 500[*]
Mexico	1993-184 Xaltocan, Mexico, kindly supplied by Dr. C. Stevenson (re-evaluated)	3.394e–5 ± 4.12e–6	0.0002629 ± 9.45e–6	5.9172e–6 ± 2.90e–6	160	1.35e–12	582 ± 109	480–650[*]

5. Application to new obsidian tools

The updated version of SIMS-SS has been applied on 13 obsidians from various parts of the world. Their SIMS H + profiles are given in Fig. 5 for Japan (same obsidian source but different cultural layers, [40]), for Greece (prefecture of Phthiotis, Islands of Andros and Youra, all from the same obsidian outcrops, Adamas and Demenegaki sources in Melos Island), and other sites around the World (Asia Minor, Chile – Rapa Nui, Hungary, Mexico). The SIMS-SS ages plotted versus the archaeological/C-14 calibrated ages are shown in Fig. 6, while Table 1 provides the calculated age parameters. Commensurability is observed between the respective ages, a verified agreement which reinforces the precision, accuracy and reliability of the SIMS-SS method, enhancing its wide applicability.

6. Conclusion

The novel SIMS-SS obsidian hydration dating method has been reassessed and suitability criteria regarding surface roughness and modelling of hydrogen profiles were established, while age calculation is made with robust new software. New age results were produced on obsidian tools from a variety of sites of the world. Dates range from a few hundreds to 30,000 years old, the latter being the oldest so far dated by the method.

References

[1] I. Friedman, R. Smith, Am. Antiquity 25 (1960) 476.
[2] J.W. Michels, L.S.T. Tsong, G.A. Smith, Archaeometry 25 (2) (1983) 107.
[3] C.M. Stevenson, I. Liritzis, M. Diakostamatiou, S.W. Novak, Mediterranean Archaeol. Archaeomet. 2 (1) (2002) 93.
[4] R.R. Lee, D.A. Leich, T.A. Tobrello, J.E. Ericson, I. Friedman, Nature 250 (1974) 44.
[5] I.S.T. Tsong et al., Science 201 (1978) 339.
[6] P. Duerden, D. Cohen, W. Ambrose, in: W. Ambrose, P. Duerden (Eds.), Archaeometry: An Australian Prospective, Australian National University, Canberra, 1982, p. 236.
[7] C.M. Stevenson, I.M. Abdelrehim, S.W. Novak, J. Archaeol. Sci. 23 (2) (2000) 233.
[8] I. Liritzis, M. Diakostamatiou, Mediterranean Archaeol. Archaeomet. 2 (1) (2002) 3.
[9] L.M. Anovitz, J.M. Elam, L.R. Riciputi, D.R. Cole, J. Archaeol. Sci. 26 (1999) 735.
[10] I. Friedman, W. Long, Science 191 (1976) 347.
[11] C.W. Meighan, L.J. Foote, P.V. Aiello, Science 160 (1968) 069.
[12] J. Kimberlin, in: R.E. Taylor (Ed.), Advances in Obsidian Glass Studies, Noyes Press, New Jersey, 1976, p. 63.
[13] C.W. Meighan, in: R.E. Taylor (Ed.), Advances in Obsidian Glass Studies, Noyes Press, New Jersey, 1976, p. 106.
[14] F.J. Findlow, V.C. Bennett, in: C.W.Meighan, P.I. Vandehoeven (Eds.), Obsidian Dates II, Institute of Archaeology Monograph VI, Los Angeles, UCLA, 1978, p.127.
[15] W.R. Ambrose, in: R.E. Taylor (Ed.), Advances in Obsidian Glass Studies, Noyes Press, New Jersey, 1976, p. 81.
[16] C.M. Stevenson, B.E. Scheetz, in: R.E. Hughes (Ed.), Current Directions in California Obsidian Studies, Contributions of the University of California Archaeological Research Facility, Berkeley, 1989, p. 23. Vol. 48.
[17] C. Stevenson, M. Gottesman, M. Macko, J. California Great Basin Antrhopol. 22 (2) (2000) 223.
[18] K.L. Hull, J. Archaeol. Sci. 28 (2001) 1025.
[19] W.R. Ambrose, C.M. Stevenson, Mediterranean Archaeol. Archaeomet. 4 (2) (2004) 5.

[20] W.R. Ambrose, S.W. Novak, I. Abdelrehim, Mediterranean Archaeol. Archaeomet. 4 (2) (2004) 17.
[21] I. Liritzis, Archaeometry 48 (3) (2006) 533.
[22] G. Braswell, Latin American Antiquity 3 (1992) 130.
[23] D.L. Nichols, T.H. Charlton, Ancient Mesoamerica 7 (1996) 231.
[24] R. Ridings, Am. Antiquity 61 (1996) 136.
[25] L. Riciputi, J.M. Elam, L.M. Anovitz, D.R. Cole, J. Archaeol. Sci. 29 (10) (2002) 1055.
[26] I. Liritzis, M. Diakostamatiou, C.M. Stevenson, S.W. Novak, I. Abdelrehim, J. Radioanal. Nucl. Chem. 261 (1) (2004) 51.
[27] I.S.T. Tsong, G.A. Smith, J.W. Michels, A.L. Wintenberg, P.D. Miller, C.D. Moak, Nucl. Instr. and Meth. B 191 (1981) 403.
[28] M. Dowsett, A. Adriaens, Nucl. Instr. and Meth. B 226 (2004) 36.
[29] I. Liritzis, M. Bonini, N. Laskaris, Surf. Interf. Anal. 40 (2008) 458.
[30] I. Liritzis, Th. Ganetsos, N. Laskaris, Mediterranean Archaeol. Archaeomet. 5 (2) (2005) 75.
[31] I. Liritzis, Th. Ganetsos, Appl. Surf. Sci. 252 (19) (2006) 7144.
[32] J. Crank, The Mathematics of Diffusion, second ed., Oxford Univ. Press, New York, 1975.
[33] D.S. Simons, in: A. Benninghoven, B. Hagenhoff, H.W. Werner (Eds.), Secondary Ion Mass Spectrometry, SIMS X. Wiley, Chichester, 1997, p. 435.
[34] I. Liritzis, N. Laskaris, M. Bonini, Phys. Stat. Sol. (c) 5 (12) (2008) 3704.
[35] S.W. Novak, G. Mahood, Cont. Mineral. Petrol. 94 (1986) 352.
[36] R.G. Wilson, F.A. Stevie, C.W. Magee, Secondary Ion Mass Spectrometry: A Practical Handbook for Depth Profiling and Bulk Impurity Analysis, Wiley, New York, 1989.
[37] S. Novak, C.M. Stevenson, Depth profiling for obsidian hydration dating. In: Fifteenth International Conference on SIMS, Manchester 12–16 September, Abstract Book (2006) 63.
[38] C.M. Stevenson, d. Wheeler, S.W. Novak, R.J. Speakman, M.D. Glascock, Archaeometry 49 (1) (2007) 153.
[39] R.H. Doremus, in: J.W. Mitchell (Ed.), Reactivity of Solids, Wiley, New York, 1969, p. 667.
[40] K. Watanabe, M. Suzuki, I. Liritzis, T. Ganetsos, S.W. Novak, N. Laskaris, K. Sasaki, N. Ikeya, Eighteenth Congress of The Indo-Pacific Prehistory Association, Manila, Philippines, 20–26 March 2006, Abstract Book.